Intermediates in Assembly by Photoactivation after Thermally Accelerated Disassembly of the Manganese Complex of Photosynthetic Water Oxidation†

Marcos Barra, Michael Haumann, Paola Loja, Roland Krivanek, Alexander Grundmeier, and Holger Dau*

Freie Universität Berlin, FB Physik, Arnimallee 14, D-14195 Berlin, Germany

Received September 4, 2006; Revised Manuscript Received October 6, 2006

ABSTRACT: The Mn_4Ca complex bound to photosystem II (PSII) is the active site of photosynthetic water oxidation. Its assembly involves binding and light-driven oxidation of manganese, a process denoted as photoactivation. The disassembly of the Mn complex is a thermally activated process involving distinct intermediates. Starting from intermediate states of the disassembly, which was initiated by a temperature jump to 47 °C, we photoactivated PSII membrane particles and monitored the activity recovery by O_2 polarography and delayed chlorophyll fluorescence measurements. Oxidation state and structural features of the formed intermediates of the Mn complex were assayed by X-ray absorption spectroscopy at the Mn K-edge. The photoactivation time courses, which exhibit a lag phase characteristic of intermediate formation only when starting with the apo-PSII, suggest that within ∼5 min of photoactivation of apo-PSII, a binuclear Mn complex is formed. It is proposed that a Mn^{III}_2(di-μ-oxo) complex is a key intermediate both in the disassembly and in the assembly reaction paths.

The light-driven formation, termed photoactivation or photoassembly (PA),[1] of the pentanuclear Mn_4Ca complex of photosystem II (PSII) is a prerequisite for photosynthetic oxygen evolution activity. Water molecules are oxidized at the Mn complex, and the atmospheric dioxygen is produced as a byproduct. The Mn complex is coordinated predominantly by amino acid residues of the D1 subunit of PSII, which is visible in the recently determined crystal structures (*1*, *2*). The D1 protein undergoes rapid turnover in intact organisms (*3*−*5*) because of its continuous damage by excess light and subsequent repair by de novo synthesis. Consequently, disassembly and light-driven assembly of the Mn complex from aqueous Mn^{2+} ions are frequent events, but they are not fully understood (*5*, *6*). Further information is required for clarification of the mechanisms in the native system but also may be important for the design of self-maintaining biomimetic compounds (artificial photosynthesis).

At variance with the assembly of the metal centers of many other metalloproteins where accessory proteins (chaperones) are involved (*7*−*9*), the formation of the Mn complex proceeds unsupported by chaperones and, in the light, solely from solvated Mn^{II} ions. Under in vitro conditions, it requires (i) the PSII protein complex depleted of Mn and Ca and comprising at least the D1/D2 core proteins and the intrinsic antenna CP47 (*10*), (ii) a medium containing Mn^{2+} (*11*, *12*), Ca^{2+} (*12*−*16*), Cl^- ions (*17*), possibly bicarbonate (*18*), and an exogenous electron acceptor (*19*), and (iii) visible light. The assembly may be more effective when complexed Mn is provided in the medium (*20*−*22*). Photoassembly of the Mn complex has been studied extensively for both continuous illumination and irradiation with light flashes (*5*, *6*). The putative intermediates formed en route to the fully assembled, functional metal site still are only insufficiently characterized.

Results for intermediates during the assembly have been reported previously (e.g., refs *5* and *23*−*26*). For a variety of experimental conditions, the recovery of O_2 evolution activity of PSII and the yield of photoactivation in previously Mn-depleted PSII samples have been studied, and these investigations have provided evidence that the photoassembly involves several sequential light and dark steps. Cheniae, Dismukes, Ananyev, Burnap, their co-workers, and other authors have developed detailed kinetic models of the photoassembly process which basically can be summarized as follows (see refs *5*, *6*, and *13* and references therein).

(1) The first light step involves photooxidation by the PSII reaction center of one Mn^{II} ion to Mn^{III} which is unstably bound. (2) By a rearrangement of the Mn^{III} species and additional binding of one Mn^{II} ion in the dark, a further unstable intermediate is formed. (3) It is transformed in the second light step to a stable Mn^{III}_2 state. (4) Subsequent binding of two more Mn ions and one Ca^{2+} ion and further light-driven Mn oxidation steps lead to the formation of the functional complex containing both Mn^{III} and Mn^{IV} species.

† Financial support from the Deutsche Forschungsgemeinschaft (SFB498, Projects C6 and C8) and from the Bundesministerium für Bildung und Forschung (Consortium "Grundlagen für einen biomimetischen und biotechnologischen Ansatz der Wasserstoffproduktion", Grant 035F0318C) is gratefully acknowledged.

* To whom correspondence should be addressed: Freie Universität Berlin, FB Physik, Arnimallee 14, D-14195 Berlin, Germany. Telephone: ++49 (0)30 8385 3581. Fax: ++49 (0)30 8385 6299. E-mail: holger.dau@physik.fu-berlin.de.

[1] Abbreviations: AAS, atomic absorption spectroscopy; chl, chlorophyll; DCIP, dichloro-*p*-indophenol; DF, delayed fluorescence; EPR, electron paramagnetic resonance; EXAFS, extended X-ray absorption fine structure; MES, morpholinoethanesulfonic acid; MW, molecular weight; PA, photoactivation; PAGE, polyacrylamide gel electrophoresis; PSII, photosystem II; SDS, sodium dodecyl sulfate; S_i, states in the catalytic cycle of water oxidation; TD, thermally induced disassembly; XANES, X-ray absorption near edge structure; XAS, X-ray absorption spectroscopy.

10.1021/bi061842z CCC: $33.50
Published on Web 11/09/2006

Notably, the rates that are coupled to each step widely may depend on the particular experimental conditions (type of PSII preparation, light intensity, concentrations of Mn^{2+}, Ca^{2+}, Cl^-, and bicarbonate ions, pH, type of buffer and exogenous electron acceptor, method for previous removal of bound Mn and Ca, and presence or absence of the extrinsic polypeptides of PSII with molecular masses of 18, 23, and 33 kDa). So far, the structure of the intermediate species and the nature of the reorganization steps have remained unclear.

Previously, we have investigated the reverse process of the assembly, namely, the inactivation and stepwise disassembly of the Mn complex by exposure of PSII to a moderate temperature increase (to 47 °C) for increasing time intervals [thermally induced disassembly (TD)] (*27*, *28*). The heat treatment procedure was chosen to specifically accelerate the usually slow disassembly process of the Mn complex so that it clearly can be discriminated from degradation of the PSII proteins. By combining oxygen polarography, X-ray absorption spectroscopy (XAS) at the Mn K-edge, EPR, and recombination chlorophyll fluorescence techniques, we have shown that the heat-induced disassembly process involves at least three steps. (1) The first most rapid step occurs within ~5 min and is coupled to the release of the extrinsic protein with a molecular mass of 18 kDa from PSII (*28*); circumstantial evidence suggested that concomitantly the affinity of the essential Ca^{2+} ion that is bound at the Mn complex (*1*, *2*, *29*, *30*) is lowered, leading to the observed inactivation of oxygen evolution (*27*, *28*). (2) In a second step, two Mn ions are reduced to Mn^{II} and released from their binding sites into the bulk within ~15 min; the remaining binuclear complex contains two Mn ions connected by a di-μ-oxo bridge (*27*). (3) The third step occurs only within hours and leads to the reduction and liberation of the remaining two Mn ions as Mn^{II} (*28*), whereby apo-PSII with an empty Mn_4Ca site is formed. In our previous investigations (*27*, *28*), whether the $Mn_2(\mu\text{-}O)_2$ intermediate formed during the heat-induced disassembly process is related to the Mn^{III}_2 state of the Mn complex which has been postulated to be formed during photoactivation remained an open question (*5*, *6*, *13*).

In the study presented here, the heat-induced dissasembly and subsequent reasssembly of the Mn complex by photoactivation are investigated. The restoration of the oxygen evolving activity is monitored by polarography and recombination chlorophyll fluorescence; the oxidation state and structural features of bound Mn are assessed by XAS.

MATERIALS AND METHODS

PSII Preparations. Highly active PSII-enriched membrane particles were prepared from market spinach as described in refs *31* and *32* and stored at −80 °C until they were used. Their O_2 evolution activity was 1200−1400 μmol of O_2 (mg of chl)$^{-1}$ h^{-1} at 28 °C as determined polarographically on a Clark-type electrode in a medium containing 10 mM NaCl, 5 mM $CaCl_2$, 1 M betaine, and 25 mM MES (pH 6) under actinic white-light illumination (410 nm < λ < 700 nm) at 28 °C (5 μg of chl/mL; 0.25 mM DCBQ and 1 mM potassium hexacyanoferrate served as artificial electron acceptors). To release the 18 and 23 kDa extrinsic proteins from PSII, a NaCl wash treatment was performed with 2.0 M NaCl in the dark according to the method described in ref *33*. To remove Mn and Ca from PSII membranes depleted of the 18 and 23 kDa proteins, samples (0.5 mg of chl/mL) were incubated on ice for 30 min in darkness under gentle stirring with 5 mM hydroxylamine (NH_2OH) (*34*) in a medium containing 10 mM NaCl, 0.4 M sucrose, and 25 mM MES-NaOH (pH 6.5) (buffer A). The NH_2OH-treated membranes were washed twice via centrifugation (40000*g* for 15 min at 4 °C) in buffer A to remove NH_2OH and finally resuspended in buffer A.

Temperature Jump Protocol. Exposure of PSII membranes to a temperature jump to 47 °C (heat treatment) was performed as outlined previously (*27*, *28*). PSII membranes originally prepared with glycine betaine (1 M) as a stabilizer present in all media were thawed on ice and washed three times in a betaine-free buffer [10 mM NaCl, 5 mM $CaCl_2$, and 25 mM MES-NaOH (pH 6)]. Then, PSII solutions (1 mg of chl/mL, 700 μL) were enclosed in Eppendorf cups and immersed in a digitally controlled water bath at 47 ± 0.5 °C. Heating for distinct time intervals was terminated by rapid cooling of samples on ice. Oxygen evolution activities were determined thereafter; either samples were subjected to the photoactivation treatments directly, or PSII membranes were collected by centrifugation (20000*g* for 10 min at 4 °C) for preparation of XAS samples. Washing after photoactivation was performed by suspending PSII membranes (~2.5 μg of chl/mL) in 300 mL of buffer A and collecting the preparation by centrifugation (40000*g* for 10 min at 4 °C).

Atomic Absorption Spectroscopy. Graphite furnace atomic absorption spectroscopy (GF-AAS) was employed for the quantification of Mn in PSII samples as described in ref *35* and carried out in the laboratory of K. Irrgang (TU-Berlin, Berlin, Germany).

Gel Electrophoresis. Polyacrylamide gel electrophoresis (PAGE) of PSII samples previously subjected to a delipidation treatment (*36*, *37*) was performed according to the method described in ref *38* using a Mini Protean II system (Bio-Rad) under the conditions described in ref *28*. Protein quantification was performed according to the method described in ref *39*.

Photoactivation Protocols. Photoactivation of PSII membranes was conducted in a buffer containing 300 mM sucrose, 35 mM NaCl, 50 mM MES-NaOH (pH 6.0), and 10 μM DCIP as an external electron acceptor. The samples (1 mL) containing 1 μM PSII [according to an estimated content of ~200 chls per reaction center (*32*)], concentrations of $MnCl_2$ indicated in the figure legends, and 5 mM $CaCl_2$ if not otherwise stated were loaded into the photoactivation cell (flat glass tray 14 mm in diameter) and incubated for 5 min in the dark. Thereafter, photoactivation was performed at room temperature (20 ± 1 °C, gentle stirring of samples) under weak continuous white light from above the cell (at a standard photon flux of 30 μE m^{-2} s^{-1} as measured at the sample surface) for designated times. After photoactivation, oxygen evolution activity immediately was determined.

Delayed Chlorophyll Fluorescence. Recombination chlorophyll fluorescence [delayed fluorescence (DF)] measurements were performed as previously described (*40*, *41*). Samples (total volume of 1.5 mL) contained 10 μg of chl/mL, 5 mM $CaCl_2$, 10 mM NaCl, 1 M betaine, and 20 μM DCBQ as the electron acceptor. Samples were photoactivated, and DF measurements were performed within ~2 min.

X-ray Absorption Spectroscopy. XAS at the Mn K-edge was performed at BESSY-II (Berlin, Germany) at double-crystal monochromator beamline KMC-1 (photon flux around 6.5 keV attenuated to $\sim 10^9$ photons s^{-1} mm^{-2}, spot size on the sample of $\sim$1 mm × $\sim$1 mm) using an energy-resolving single-element germanium detector (Canberra, active area of $\sim$1 cm^2) for detection of the excited X-ray fluorescence, digital signal processing for pulse detection (DXP from XIA), and a liquid helium-cooled cryostat with a height-adjustable sample rod (Oxford). In comparison to previous experiments, an improved detector−cryostat arrangement was used. To prevent absorption of the X-ray fluorescence by an intervening gas layer and to maximize the solid angle for X-ray detection, the detector head was included in the thermal insulation vaccum of the cryostat. The resulting sample−detector distance had been $\sim$3 cm (from the center of the sample to the center of the detector). A chromium foil (10 μm) in front of the detector largely suppressed scattered X-rays so that detector saturation was kept well below a level of 20% at a total count rate of $\sim 10^5$ s^{-1}. The pulses at the DXP output, which are proportional to the Mn K_α fluorescence yield, were detected in a single-channel analyzer window centered around 5900 eV and counted by the beamline electronics. XAS measurements were performed, at 10 K, by scanning of the monochromator (Si111 crystals, scan range of 6500−7200 eV). X-ray fluorescence signals were corrected for detector saturation using the total count rate delivered by the DXP. The energy axis of XAS spectra was corrected according to the position of the narrow pre-edge peak at 6543.3 eV of a $KMnO_4$ standard measured simultaneously in absorption mode (*31*, *42*). Spectra were normalized as described in ref *43*, and up to 15 scans, each performed on a separate spot of the samples, were averaged. The given K-edge energies were determined by the "integration method" outlined in ref *43*. XAS samples were prepared by filling $\sim$20 μL of pellets of previously heated, photoactivated PSII membrane samples (see figure legends), which previously had been collected by centrifugation, into acrylic glass sample holders covered on one side with Kapton foil. Subsequently, the samples were frozen in liquid nitrogen. The Mn concentration in the XAS samples was $\sim$200 μM in control PSII membrane samples and lower in the photoactivated preparations. EXAFS spectra were extracted, and simulations were performed by least-squares curve fitting of k^3-weighted oscillations in the *k*-space as previously described (*43*) using phase functions calculated by Feff-7 (*59*). For further details of the applied procedure of EXAFS data analysis, see refs *43* and *50*.

RESULTS AND DISCUSSION

Thermally Induced Stepwise Disassembly. PSII samples were exposed to a temperature of 47 °C for increasing time intervals, and thereafter, the oxygen evolution activity was determined by polarography. Figure 1 shows that the decrease in the O_2 activity (○) exhibits three kinetic components. A rapid phase (rate constant $k_1 = 0.8$ min^{-1}), accounting for the loss of more than 60% of the control activity, was terminated already after heating for $\sim$5 min. Then, O_2 activity decreased $\sim$10 times more slowly ($k_2 = 0.08$ min^{-1}); this phase was terminated after heating for $\sim$15−20 min. The decrease in the remaining small offset activity of $\sim$8% was not completed ($k_3 = 0.008$ min^{-1}) in the heating time interval of 120 min.

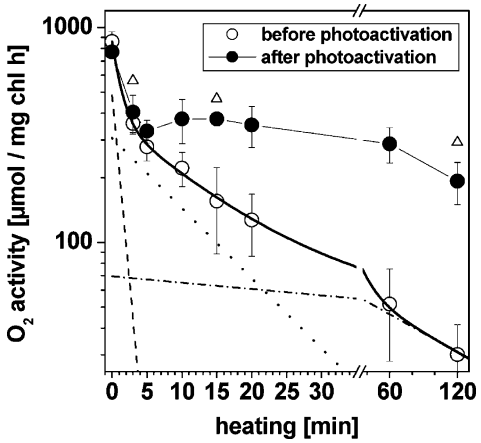

FIGURE 1: Decrease in the oxygen evolution activity of PSII membrane samples during heating to 47 °C (○) and activity in the same samples after subsequent photoactivation for 60 min (●). Three data sets have been averaged, and error bars denote standard deviations; 5 mM Ca^{2+} was present in the samples. Open triangles represent data of photoactivated samples measured at 20 mM Ca^{2+} which are shown for comparison. The solid line represents a triple-exponential simulation with parameters given in the text; the broken lines show the individual contributions of the three kinetic components.

The most rapid phase of the decrease of the O_2 activity is associated with the concomitant release of the extrinsic polypeptide with a molecular mass of 18 kDa from PSII (*28*). Already after heating of PSII for 3 min, the 18 kDa protein was almost undetectable by gel electrophoresis, whereas the 23 kDa protein remained mostly bound as revealed by comparison with control PSII samples and samples in which both the 18 and 23 kDa extrinsic proteins quantitatively were removed from PSII by a NaCl wash procedure (data not shown; see ref *28*). The second phase of the O_2 activity decrease reflects the release of two Mn ions of the Mn_4 complex as Mn^{II} into the medium as previously shown by AAS, EPR, and X-ray absorption spectroscopy (*27*, *28*), thereby causing almost complete inactivation of O_2 production. The offset activity of $\sim$8% may be due to side reactions at the PSII donor side involving peroxide and reoxidation of previously reduced DCBQ molecules as this offset further was diminished, but the more rapid phases were unchanged, when the ferricyanide concentration was increased from 1 to 5 mM and DCBQ was omitted from the O_2 activity assay (not shown).

Photoactivation Starting at Various Disassembly Stages. PSII samples heated for increasing time intervals were subjected to a photoactivation procedure (see Materials and Methods) for 60 min, employing weak white light illumination and the addition to the samples of approximately stoichiometric amounts of Mn^{II} per PSII reaction center (4 Mn atoms per 200 chls). The resulting O_2 activities are shown in Figure 1 as solid circles. The diminished O_2 activity observed in PSII samples which were heated for less than $\sim$5 min could not be increased by illumination. For heating intervals between 5 and 20 min, photoactivation increased the activity to an approximately constant value of $\sim$400 μmol of O_2 (mg of chl)$^{-1}$ h^{-1}. Apparently, the presence of stoichiometric amounts of Mn^{II} (and of superstoichiometric Ca^{2+}) in the photoactivation mixture was sufficient to restore

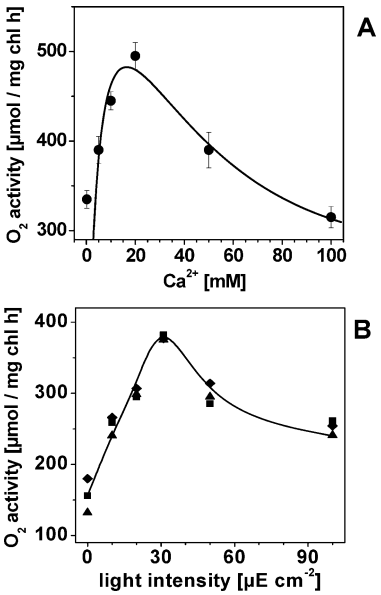

FIGURE 2: (A) O_2 activity of PSII membranes heated for 3 min (●) as a function of Ca^{2+} concentration in the assay medium. Three data sets have been averaged; error bars denote standard deviations. The solid line represents a simulation using Michaelis−Menten type binding kinetics with a K_D of 4.2 mM to account for the activity increase at increasing Ca^{2+} concentrations which is counteracted by a decay of the activity described by a single-exponential function using a half-inhibition Ca^{2+} concentration of 31.4 mM. (B) O_2 activity in PSII membranes heated for 15 min and subsequently photoactivated for 60 min at the indicated light intensities. Three data sets are shown; the line has been drawn to guide the eye.

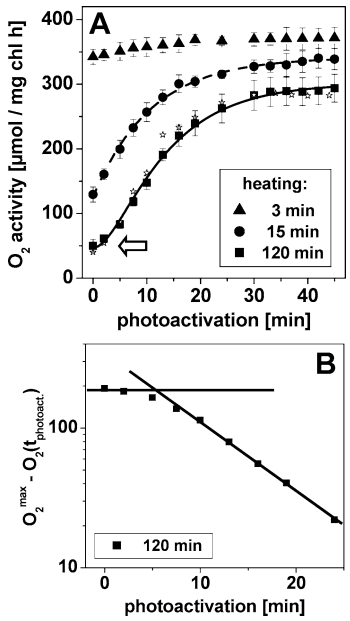

FIGURE 3: (A) Time courses of photoactivation after previous heat deactivation for the indicated time periods. The data points represent the average of three experiments (error bars denote the standard deviation). The dashed line is the single-exponential simulation, and the solid line is the simulation using a consecutive reaction scheme (*27*); for the parameters, see the text. Asterisks denote activities measured on samples that were depleted of the 18 and 23 kDa extrinsic proteins by a NaCl wash procedure, then depleted of Mn and Ca by reduction with hydroxylamine (NH_2OH), and subsequently photoactivated. The arrow points to the lag phase with a duration of ∼5 min in the recovery of O_2 activity. (B) Semilogarithmic plot of the data for the 120 min photoactivation. Lines have been drawn to emphasize the deviation from the linear behavior which is expected in the absence of a lag phase.

the activity to a value similar to that observed in the PSII samples depleted of the 18 kDa protein by heating for ∼5 min. For longer heating times of up to 120 min, a similar activity was still reached after photoactivation. Clearly, the heat-treated PSII was able to serve as the starting material for photoactivation.

Previous XAS studies and measurements of recombination chlorophyll fluorescence transients [the so-called delayed fluorescence (*40*)] suggested that the loss of the 18 kDa protein in samples heated for a short time (≤5 min) is accompanied by a diminished affinity of the essential Ca^{2+} ion for its binding site at the Mn complex (*27*, *28*). Measurements of the O_2 activity of samples heated for 3 min and subsequently photoactivated in the presence of various Ca^{2+} concentrations in the assay medium revealed a low activity in the absence of additional Ca^{2+} (i.e., at a residual Ca^{2+} concentration of ∼150 μM) and an apparent activity increase by a factor of ∼1.5 at an optimum Ca^{2+} concentration of 20 mM in the medium (Figure 2A). At higher concentrations, Ca^{2+} became inhibitory, possibly because such conditions affected the binding properties of the 23 and 33 kDa extrinsic proteins in a fraction of the PSII centers (*15*, *44*). In the absence of any inhibitory effect of high Ca^{2+} concentrations, an activity similar to the one observed in the unheated controls might be attained. These results are compatible with our previous notion (*27*, *28*) that the diminished affinity for Ca^{2+}, likely brought about by the loss of the 18 kDa protein, is the primary cause for the lowered O_2 activity in PSII heated for a short time.

EXAFS measurements at the Mn K-edge have revealed that after samples have been heated for ∼15−20 min a binuclear Mn complex is formed in which the two Mn ions still are connected by a di-μ-oxo bridge (*27*). As is clearly visible in Figure 1, PSII samples heated for 15−20 min could be photoactivated; the reached activity was similar to that in samples heated for less than 5 min. The straightforward interpretation of this result is that the Mn_2 complex formed after heating for 15−20 min can serve as a starting state in the photoactivation process. The maximally achievable activity depended on the light intensity during photoactivation (Figure 2B). Optimal activities after photoactivation of samples heated for 15 min (and also for 120 min, not shown) were observed at ∼30 μE m^{-2}. For photoactivation after Mn depletion, similar optimal light intensities have been reported (*13*, *16*, *45*). After samples were heated for 120 min, most Mn ions were released from PSII as Mn^{II} (see below and ref *28*). Clearly, the thereby formed apo-PSII also was functional in photoactivation (Figure 1).

Kinetics of Photoactivation in Previously Heated Samples. We explored the time course of the photoactivation process in PSII samples which were exposed previously to the heat treatment. The O_2 activity in PSII heated for 3 min was approximately independent of the photoactivation time [Figure 3(▲)], in line with the absence of release of Mn from PSII heated for a short time (*27*). In samples heated for 15 min, on the other hand, the activity increased during the photoactivation and reached a constant level after ∼40 min [Figure 3 (●)]. The increase was described well by a single-exponential function with a rate constant (k_{A2}) of 0.095 min^{-1} (line). In samples heated for 120 min, the increase in activity was not monophasic. Rather, during the first 5 min of

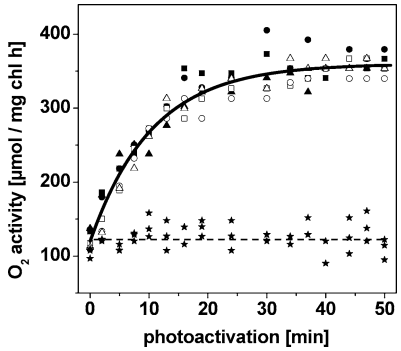

FIGURE 4: Time courses of the recovery of O_2 activity during photoactivation in PSII samples previously heated for 15 min. Solid symbols depict three data sets from PSII samples that, after heating, were photoactivated in the absence of additional Mn. Open symbols depict data for one washing step after heating to remove unbound Mn, and subsequent photoactivation after the addition of two Mn^{II} ions per PSII to the medium. Asterisks depict data for one washing step after heating to remove unbound Mn and photoactivation without additional Mn. The solid line represents a single-exponential simulation with a k_{A2} of 0.095 min^{-1}.

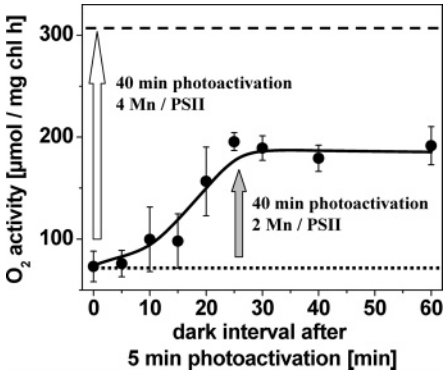

FIGURE 5: Final O_2 activities in PSII membranes that were heated for 2 h and washed to remove unbound Mn. Thereafter, samples were photoactivated for 5 min with two Mn ions per PSII at increasing intervals of dark incubation on ice prior to the final photoactivation for 40 min (●). The dashed line represents the activity after photoactivation with four Mn ions per PSII. For further details, see the text.

photoactivation, a lag phase (arrow) was observed during which the activity remained low, and only thereafter did an apparently monophasic activity increase occur [Figure 3 (■)]. Such a time course suggested that the photoactivation involved at least two sequential steps. Indeed, using a consecutive reaction scheme (*27*) and employing an apparent rate constant k_{A1} of 0.25 min^{-1} ($t_{1/2}$ = 2.8 min) to account for the lag phase and the above rate of 0.095 min^{-1} ($t_{1/2}$ = 7.3 min) for the monophasic increase yielded a satisfying description of the data points [Figure 3A (—)]. Monitoring photoactivation in samples depleted of Mn was achieved by a reductive treatment in the presence of hydroxylamine (NH_2-OH) followed by a washing step to remove the liberated Mn^{II} ions which revealed that the lag phase behavior was not a specific property of the PSII heated for long times but could also be observed in apo-PSII samples produced by reductive Mn removal [Figure 3 (∗)].

In summary, the time course of the photoactivation suggests that, when apo-PSII with an unoccupied Mn binding site is employed as the starting material, within ∼5 min an intermediate state of the Mn complex is formed which is inactive in O_2 evolution. Subsequently, in a slower reaction, the functional Mn_4 complex is assembled. Both steps require the input of light energy. When the presumably binuclear Mn complex (see below) is used as the starting point, photoactivation to yield the Mn_4 complex occurs without a lag phase. These results can be explained by assuming that the intermediate formed after photoactivation of apo-PSII for ∼5 min corresponds to the same binuclear Mn complex that is formed in the disassembly process after heating for ∼15 min.

Mn Requirement for Reassembly of the Mn_2 Complex. In samples heated for 15 min, the release of approximately two of the four Mn ions of the complex as Mn^{II} to the suspending medium has been observed; two Mn ions remain bound to PSII (*27*, *28*). Such samples were subjected to the photoactivation procedure in the absence of additional Mn, meaning that the two bound ions and the two ions released into the medium still were present. The initial activity of these samples increased monophasically during photoactivation (Figure 4, filled symbols) to a value that was similar to that of samples heated for only 3 min (Figure 3), which contain four Mn ions bound to PSII. Seemingly, the liberated Mn^{II} ions were reincorporated into the complex during photoactivation so that the O_2-evolving Mn_4 site was recovered to almost 100%. When the samples heated for 15 min subsequently were washed to remove all unbound or loosely bound Mn ions, photoactivation in the absence of added Mn was not possible [Figure 4 (∗)]. Thus, there was no detectable redistribution of the two bound Mn ions among the PSII reaction centers. However, activity was almost fully regained if two Mn^{II} ions per PSII reaction center after washing were added to the photoactivation medium (Figure 4, open symbols). The two Mn ions remaining after a heating period of 15 min are bound relatively firmly to PSII, in accord with previous observations (*27*, *28*).

Stability of the Mn_2 Intermediate of Photoactivation. The stability of the state that had been formed after photoactivation for only 5 min (i.e., during the lag phase; see Figure 3) was studied, starting with apo-PSII created by heating for 2 h and subsequent washing to remove the liberated Mn ions. Such PSII membranes were photoactivated for 5 min in the presence of two Mn atoms per PSII center, thereafter incubated for increasing time intervals in the dark, and subsequently photoactivated for 40 min. The resulting O_2 activities are depicted in Figure 5 (●). With a duration of up to ∼15 min of the intervening dark interval, (1) the final activity remained low (at its background level) but (2) for a longer dark interval of up to 60 min increased by a value [∼120 μmol of O_2 (mg of chl)$^{-1}$ h^{-1}] that was approximately half of the increase obtained after photoactivation with four Mn atoms per PSII center [∼240 μmol of O_2 (mg of chl)$^{-1}$ h^{-1} (− − −)]. If the PSII membranes were collected by centrifugation after photoactivation for 5 min with two Mn atoms per PSII, resuspended, supplied with two additional Mn atoms per PSII center (duration of the whole procedure of ∼15 min), and then photoactivated for 40 min, the gain in activity was ∼70% [∼180 μmol of O_2 (mg of chl)$^{-1}$ h^{-1}] of that obtained after photoactivation with four Mn atoms per PSII.

The results described above suggest that the two Mn ions that become bound to PSII within 5 min of photoactivation remain bound for ∼15 min in the dark (and also for 40 min in the light). For longer dark exposure times, these two Mn

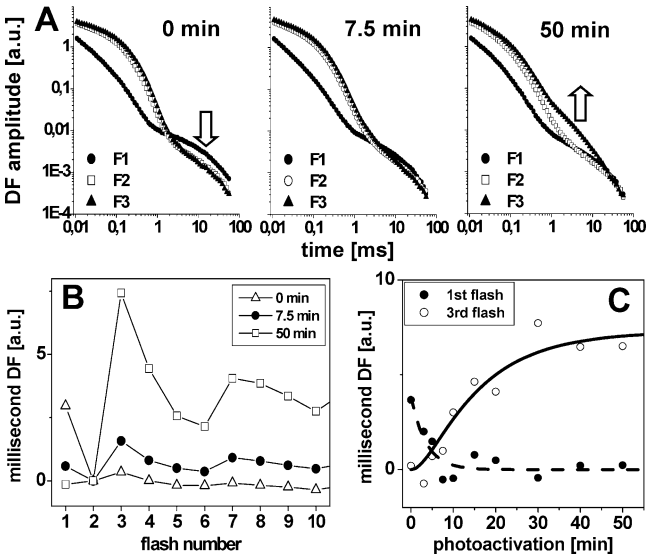

FIGURE 6: Results of delayed chl fluorescence (DF) measurements on heated and photoactivated PSII. (A) DF transients measured after illumination by one, two, or three laser flashes applied to apo-PSII samples that previously had been photoactivated for 0, 7.5, and 50 min in the presence of four Mn ions per PSII. The arrows denote the kinetic phases that decreased in amplitude on flash 1 and increased on flash 3 with increasing photoactivation periods. Three transients from independent samples were averaged on each flash. (B) Mean DF amplitudes from averaging between 2 and 10 ms after each flash in a series. The three data sets have been normalized to zero on the DF amplitude on flash 2. (C) DF amplitudes in the millisecond time range as a function of the duration of photoactivation on flashes 1 (●) and 3 (○). From all DF amplitudes, a small offset value needed to set the transient on the second flash of the series to zero was subtracted. The dashed line represents a single-exponential decay with a time constant ($k_{A1'}$) of 0.27 min^{-1}, and the solid line was derived from a simulation using a consecutive reaction scheme (*27*), the above value of $k_{A1'}$, and a $k_{A2'}$ of 0.073 min^{-1}.

ions are released, possibly cooperatively, to the medium. Only after this Mn release are centers with four Mn atoms formed in approximately half of the PSII population in the subsequent 40 min photoactivation procedure. The difference between the state (apo-PSII + 2Mn in the medium) that is expected to be present both in case 1, i.e., prior to the photoactivation steps without an intervening dark interval, and in case 2, reached after the 60 min dark interval after photoactivation for 5 min but prior to the 40 min photoactivation, is the long dark incubation time in case 2. Apparently, by this incubation, the PSII−Mn_2 state that is formed after photoactivation for 5 min is destabilized so that the two Mn ions are redistributed among the PSII centers, resulting in the formation of an active PSII−Mn_4 complex in half of the centers. At present, the nature of the destabilization effect is unclear. In any event, besides providing insights into the stability of the Mn_2 intermediate, these findings open up the way to spectroscopic studies on the binuclear intermediate (described further below).

DF Measurements Confirm Intermediate Formation. The formation of a partially assembled Mn complex after photoactivation for only 5 min may suggest that the bound Mn could function as an electron donor to the oxidized tyrosine Z (Y_Z^{ox}) formed upon flash excitation of the sample (*28*, *46*, *47*). This option was explored by measurements of the decay of delayed chlorophyll fluorescence (DF) (*40*, *41*) after laser flash excitation (Figure 6). Prior to photoactivation, i.e., in the absence of bound Mn, the DF transient on flash 1 decayed more rapidly than on the following flashes (Figure 6A, 0 min) as expected for oxidation of Y_Z by P_{680}^+ only on flash 1 in tens of microseconds (*28*, *47*) and charge recombination between P_{680}^+ and Q_A^- occurring on the following flashes in the time range of hundreds of microseconds (*28*, *47*). During the first few minutes of photoactivation, there was a decrease in the DF amplitude induced by flash 1 in the millisecond time range (Figure 6A, 7.5 min), but the DF transients on higher flash numbers were almost unchanged. Accordingly, on the higher flashes, charge recombination still was the dominating process. However, the decreased DF amplitude on flash 1 is compatible with partial reduction of Y_Z^{ox} by the Mn_2 complex on the millisecond time scale. After photoactivation for 50 min, there was a pronounced DF phase with a decay half-time of ~1.1 ms on flash 3 (Figure 6A, 50 min). This phase is related to Y_Z^{ox} reduction during O_2 formation on the $S_3 \rightarrow S_0$ transition as previously shown (*41*, *48*).

Figure 6B shows the mean DF amplitudes as obtained by averaging from 2 to 10 ms after each flash in samples photoactivated for increasing time intervals. Even after photoactivation for 50 min and a subsequent dark interval of only ~1 min prior to the measurements, PSII seems to be almost dark-adapted prior to the laser flashes. The Mn complex predominantly was in its S_1 state, as there is a pronounced quaternary oscillation in the DF amplitudes related to the O_2-evolving step first occurring on flash 3. As shown in Figure 6C, the millisecond amplitude measured after the first flash decreases within the first 10 min of photoactivation possibly due to the transfer of an electron from the Mn_2 intermediate as discussed above. The amplitude of the O_2 phase measured after the third flash may exhibit a lag phase prior to its rise. The lag phase duration was similar to that observed in the increase in O_2 activity during photoactivation (see Figure 3) and confirms intermediate formation. Apparently, the amplitude decrease on flash 1 ($k_{A1'}$ = 0.27 min^{-1}) was completed within the duration of the lag phase observed for the flash 3 signal. The amplitudes on flash 3 were simulated well using the consecutive reaction scheme (*27*) and the same rate constant $k_{A1'}$ to account for the lag and a $k_{A2'}$ rate of 0.073 min^{-1} accounting for the rise (Figure 6C, lines). The obtained rate constants, within error, are similar to those obtained from the O_2 evolution measurements (see Figure 3).

In conclusion, the DF results support the notion that an intermediate is formed within the first few minutes of the photoactivation process. This intermediate may be able to donate an electron to the $Y_Z^{\bullet+}$ radical.

X-ray Absorption Spectroscopy. X-ray absorption spectra at the Mn K-edge were measured on samples which were heated and subsequently photoactivated in the presence of stoichiometric amounts of Mn (Figure 7). Control PSII (no heating, no photoactivation) exhibited a XANES spectrum (Figure 7A, thick line) that, as judged by the K-edge energy of 6551.4 eV, is attributable to the Mn complex in its dark stable S_1 state (*42*). Apo-PSII that was photoactivated for 40 min in the presence of four Mn atoms per PSII (and thereafter active in O_2 evolution) and collected by centrifugation exhibited a similarly shaped XANES spectrum (dashed line) and a slightly lower edge energy of 6551.1 eV, still compatible with the predominant presence of the S_1 state

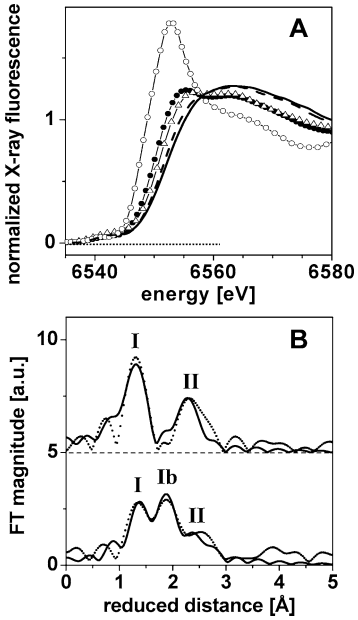

FIGURE 7: (A) XANES spectra at the manganese K-edge. The solid line is for control PSII with the Mn complex in its S_1 state (no heating, no washing, no photoactivation). The empty circles are for PSII samples heated for 2 h (no washing, no photoactivation). The dashed line is for samples photoactivated for 40 min with four Mn ions per PSII. The empty triangles are for samples heated for 15 min and subsequently washed to remove unbound Mn (no photoactivation). The filled circles are for samples heated for 2 h, washed to remove unbound Mn, and photoactivated for 5 min in the presence of two Mn ions per PSII. (B) Fourier transforms (FTs, dots) of k^3-weighted EXAFS oscillations of samples photoactivated for 40 min with four Mn ions per PSII (top) and for 5 min with two Mn ions per PSII (bottom). FTs were calculated using a k range of 2.1−11.2 Å^{-1} and cosine windows extending over 10% of the k range at high and low k values. Solid lines represent simulated spectra calculated with parameters listed in Table 1. In panel B, spectra are vertically displaced by 5 units for better comparison.

and admixtures of minor portions of lower oxidation states of the Mn_4 complex and of aqueous Mn^{II}. In both samples, the Mn complex predominantly seems to be present in its mean oxidation state of +3.5 of the S_1 state that can be assigned to a $Mn^{III}_2Mn^{IV}_2$ complex (*42*, *49*). The XANES spectrum of hexaquo Mn^{II} {$[Mn^{II}(H_2O)_6]^{2+}$ complex} is shown for comparison in Figure 7A (○; E_{edge} = 6547.2 eV). Samples that were heated for 15 min and subsequently washed to remove unbound Mn displayed a XANES spectrum [Figure 7A (△)] which may be attributable to Mn^{III} (E_{edge} = 6550.1 eV). This estimate is based on an edge shift of −0.6 to −0.8 eV per single-electron reduction of the Mn_4 complex initially in its S_1 state (*31*, *50*). Hence, the binuclear Mn complex formed after samples were heated for 15 min presumably may be in the Mn^{III}_2 oxidation state, in accord with previous estimates (*27*). Samples that were heated for 120 min, washed for removal of unbound Mn, subsequently photoactivated in the presence of two Mn atoms per PSII for only 5 min, that is for the duration of the lag phase observed in the photoactivation time course (see Figures 3 and 6), and collected by centrifugation exhibited a XANES spectrum [Figure 7A (●); E_{edge} = 6549.6 eV] which also is compatible with a major contribution from Mn^{III}. A minor but significant contribution of Mn^{II}, accounting for the relatively low edge energy, is apparent from the larger primary maximum of the edge. Such a Mn^{II} contribution was expected and also is visible in the EXAFS spectrum (see below), because the intermediate formed after photoactivation for 5 min exhibited only limited stability (compare Figure 5) and was in part degraded during collection of the PSII membranes by centrifugation and preparation of the EXAFS samples.

The Fourier transforms (FTs) of EXAFS spectra from samples previously heated for 2 h, washed, and then collected by centrifugation after photoactivation for 40 min with four Mn atoms per PSII (top) or for 5 min with two Mn atoms per PSII (bottom) are shown in Figure 7B (dots). The top spectrum revealed two major peaks (I and II) which is typical for the Mn complex of PSII (*49*−*52*). Peak I is attributable to direct O/N ligands to Mn, and peak II mainly reflects Mn−Mn distances of ∼2.7 Å (*50*). A simulation of the spectrum employing three shells of backscatterers [two O/N shells to account for the complex distance distribution in the first coordination sphere of Mn (*42*, *50*) and one Mn−Mn vector ∼2.7 Å in length] yielded a result (Table 1) that was similar to previous ones obtained from simulations of EXAFS spectra of the native Mn complex in its S_1 state (*42*, *50*). [Longer Mn−Mn/Ca vectors (*27*, *42*, *43*) were neglected because of the sizable noise level of the spectra due to a comparably low Mn concentration of ∼140 μM in samples photoactivated for 40 min and of ∼45 μM in samples photoactivated for 5 min, as estimated from the X-ray fluorescence counts due to Mn.] Thus, the overall structure of the functional Mn complex created by photoactivation in vitro and of the native Mn complex appears to be similar, as expected. In particular, there is approximately one Mn−Mn vector ∼2.7 Å in length per Mn ion (N_{Mn-Mn} close to unity) in both cases, meaning that at least two pairs of Mn ions which each are connected by a di-μ-oxo bridge are present (*27*, *42*, *43*, *50*). That the value of N_{Mn-Mn} exceeded unity is attributable to the neglect of Mn−metal distances larger than ∼2.7 Å in the simulation approach (*42*, *50*).

In the spectrum of samples which have been photoactivated for only 5 min with two Mn atoms per PSII, three FT peaks are apparent (Figure 7B, bottom). The new peak Ib, according to the simulation results (Table 1), is attributable to Mn^{II} in water [typical Mn−O(H_2) distance of ∼2.18 Å (*26*, *54*, *55*)]. The Mn^{II} contribution also was inferred from the XANES spectrum. More interesting is the presence of Mn−Mn distances in the range of 2.7−3 Å (peak II). Simulations revealed that the number of ∼2.7 Å distances per Mn ion was reduced (by at least 30%) compared to the number in samples photoactivated for 40 min. We note that, due to the low Mn concentrations, the quality of the data was relatively low so that the coordination number is highly uncertain. In any event, the data are compatible with the presence of a significant fraction of centers containing Mn ions connected by a di-μ-oxo bridge. (Longer Mn−Mn distances also may be present, resulting from Mn ions connected by a mono-μ-oxo bridge or by di-μ-OH bridges due to partial degradation of the intermediate, which were not analyzed further.) Thus, the results of the polarographical photoactivation studies and XAS data analysis suggest formation of a binuclear Mn complex within the first few minutes of photoactivation. This complex may contain a Mn^{III}_2(di-μ-oxo) motif. A similar site is formed after a 15 min heat treatment as shown in ref *27*. This binuclear center may represent a relatively stable intermediate both in the

Table 1: Simulation Results of a Joint Fit (*27*) of the Two EXAFS Spectra Shown in Figure 7B[a]

	N_i (per Mn), R_i (Å), $2\sigma_i^2$ (Å^2)		
	Mn−O shell	Mn−O shell	Mn−Mn shell
40 min photoactivation, 4 Mn	4.8, 1.85, 0.018	0.7, 2.18, 0.018	1.1, 2.73, 0.006
5 min photoactivation, 2 Mn	3.1, 1.85, 0.002	2.4, 2.18, 0.002	0.8, 2.74, 0.006

[a] N_i is the coordination number. R_i is the Mn−ligand distance. $2\sigma_i^2$ is the Debye−Waller parameter. The following restraints have been used in the simulations. The sum of the two N_{Mn-O} values was set to 5.5, and the two R_{Mn-O} and $2\sigma_{Mn-O}^2$ values were coupled in the simulation to yield the same values for both spectra. For both spectra, the same fixed value of $2\sigma_{Mn-Mn}^2$ was employed. The R_F value [error sum (*58*)] of the joint fit was 37%, calculated over a reduced distance range of 1−3 Å.

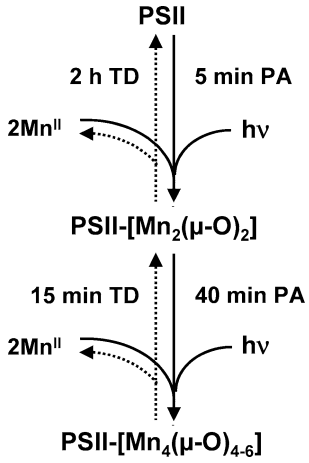

FIGURE 8: Kinetic scheme of the processes proposed to occur during the thermally induced disassembly (TD) of the Mn complex and its subsequent reassembly by photoactivation (PA).

thermally induced disassembly and in the photoactivation process of the Mn complex.

CONCLUSIONS

On the basis of previous investigations (*27*, *28*) and this investigation, a sequence of events in the thermally accelerated disassembly (TD) and subsequent reassembly of the Mn complex by photoactivation (PA) is proposed which is presented in Figure 8. As shown in ref *27*, after samples are heated for ∼15 min, most likely a $Mn_2(\mu\text{-}O)_2$ complex (suggested by a Mn−Mn distance of 2.7 Å) is formed, whereas the other two Mn ions are in the Mn^{II} oxidation state and presumably released to the bulk phase. In the study presented here, we provide evidence that the binuclear Mn complex obtained after heating for ∼15 min can be transformed by photoactivation to the functional tetramanganese complex of PSII if two additional Mn^{II} ions are present in the medium.

When apo-PSII created by the extraction of Mn either by prolonged heating or by biochemical extraction is used as the starting material, a lag phase of 5−10 min in the recovery of O_2 activity during photoactivation suggests formation of an assembly intermediate. However, for photoactivation of the $Mn_2(\mu\text{-}O)_2$ centers obtained after an ∼15 min heating, no lag phase is observable. This finding suggests that the binuclear Mn complex formed by heating corresponds to the assembly intermediate. This hypothesis is compatible with the XAS data obtained for PSII photoactivated for 5 min. Therefore, we propose that there is a binuclear intermediate in the disassembly as well as in the photoactivation process which contains two Mn ions connected by a di-μ-oxo bridge.

We note that the binuclear Mn complex obtained (1) after heating of intact PSII for ∼15 min is more stable than the one formed (2) by photoactivation after a 2 h heat treatment which in turn is more stable than that (3) observed after a second photoactivation following dark incubation for 1 h after a previous short photoactivation of PSII heated for 2 h. The increased level of destabilization of the Mn_2 complex in response to the harsher treatments of the PSII membranes may be attributable to structural changes at the PSII donor side which facilitate the reduction of the high-valent Mn ions of the binuclear complex by reduced electron acceptor molecules (*25*). Partial unfolding or structural rearrangements of the 23 and 33 kDa proteins possibly are involved. Further experiments are required to clarify the nature of the destabilization effect.

Previous investigations have provided evidence of a state in which two Mn ions are bound to PSII during photoactivation (see refs *5*, *24*, and *45* and references therein). The proposed $Mn_2(\mu\text{-}O)_2$ intermediate in the light-driven assembly and thermally activated disassembly may correspond to intermediates postulated by other authors (e.g., states "IM_2" in ref *24* and "D" in ref *45*). The formation of intermediates containing two Mn ions also previously has been reported after chemical reduction of PSII or partial removal of the extrinsic polypeptides (see refs *6* and *61*−*63* and references therein). However, structural information about these intermediates is insufficient or not available so that their relation to the Mn_2 state formed by short time photoactivation as characterized in this investigation needs to be verified. In any event, the results of this study and previous investigations suggest that a binuclear state is a key intermediate both in the assembly and in the disassembly of the Mn complex.

We hypothesize that, in vivo, the formation of a functional Mn complex after direct or indirect photodamage may occur not only by de novo synthesis of the D1 protein of PSII and subsequent photoactivation but also by immediate light-driven repair. After photodamage and loss of the two loosely bound Mn ions from PSII, a light-driven reassembly could result in a fully functional Mn complex. Similar self-maintenance mechanisms may well be a prerequisite for long-term stability of biomimetic systems which are aiming at artificial photosynthesis (along with further requirements derived from PSII function; see, e.g., refs *56*, *57*, and *60*).

ACKNOWLEDGMENT

We thank Dr. F. Schäfers and M. Mertin at BESSY for excellent support in the XAS measurements, Dr. P. Liebisch for his contributions to XAS data collection, Dr. K. Irrgang (TU-Berlin) and S. Löscher from our workgroup for help in the AAS measurements, and M. Fünning for skillful technical assistance.

REFERENCES

1. Loll, B., Kern, J., Saenger, W., Zouni, A., and Biesiadka, J. (2005) Towards complete cofactor arrangement in the 3.0 Å resolution structure of photosystem II, *Nature 438*, 1040−1044.
2. Ferreira, K. N., Iverson, T. M., Maghlaoui, K., Barber, J., and Iwata, S. (2004) Architecture of the photosynthetic oxygen-evolving center, *Science 303*, 1831−1838.
3. Zhang, L., and Aro, E. M. (2002) Synthesis, membrane insertion and assembly of the chloroplast-encoded D1 protein into photosystem II, *FEBS Lett. 512*, 13−18.
4. Barber, J., and Andersson, B. (1992) Too much of a good thing: Light can be bad for photosynthesis, *Trends Biochem. Sci. 17*, 61−66.
5. Burnap, R. L. (2004) D1 protein processing and Mn cluster assembly in light of the emerging photosystem II structure, *Phys. Chem. Chem. Phys. 6*, 4803−4809.
6. Ananyev, G. M., Zaltsman, L., Vasko, C., and Dismukes, G. C. (2001) The inorganic biochemistry of photosynthetic oxygen evolution/water oxidation, *Biochim. Biophys. Acta 1503*, 52−68.
7. Tottey, S., Harvie, D. R., and Robinson, N. J. (2005) Understanding how cells allocate metals using metal sensors and metallochaperones, *Acc. Chem. Res. 38*, 775−783.
8. Rosenzweig, A. C. (2002) Metallochaperones: Bind and deliver, *Chem. Biol. 9*, 673−677.
9. O'Halloran, T. V., and Culotta, V. C. (2000) Metallochaperones, an intracellular shuttle service for metal ions, *J. Biol. Chem. 275*, 25057−25060.
10. Büchel, C., Barber, J., Ananyev, G. M., Eshagui, S., Watt, R., and Dismukes, G. C. (1999) Photoassembly of the manganese cluster and oxygen evolution from monomeric and dimeric CP47 reaction center photosystem II complexes, *Proc. Natl. Acad. Sci. U.S.A. 96*, 14288−14293.
11. Cheniae, G. M., and Martin, I. F. (1971) Photoactivation of manganese catalyst of O_2 evolution. 1. Biochemical and kinetic aspects, *Biochim. Biophys. Acta 253*, 167−181.
12. Miller, A. F., and Brudvig, G. W. (1989) Manganese and calcium requirements for reconstitution of oxygen-evolution activity in manganese-depleted photosystem II membranes, *Biochemistry 28*, 8181−8190.
13. Chen, G., Kasimir, J., and Cheniae, G. M. (1995) Calcium modulates the photoassembly of photosystem II $(Mn)_4$-clusters by preventing ligation of nonfunctional high-valency states of manganese, *Biochemistry 34*, 13511−13526.
14. Ananyev, G. M., and Dismukes, G. C. (1997) Calcium induces binding and formation of a spin-coupled dimanganese(II, II) center in the apo-water oxidation complex of photosystem II as precursor to the functional tetra-Mn/Ca cluster, *Biochemistry 36*, 11342−11350.
15. Ananyev, G. M., and Dismukes, G. C. (1996) High-resolution kinetic studies of the reassembly of the tetra-manganese cluster of photosynthetic water oxidation: Proton equilibrium, cations, and electrostatics, *Biochemistry 35*, 14608−14617.
16. Tamura, N., Inoue, Y., and Cheniae, G. M. (1989) Photoactivation of the water-oxidizing complex in photosystem II membranes depleted of Mn, Ca and extrinsic proteins: 2. Studies on the functions of Ca^{2+}, *Biochim. Biophys. Acta 976*, 173−181.
17. Miyao, M., and Inoue, Y. (1991) Enhancement by chloride ions of photoactivation of oxygen evolution in manganese-depleted photosystem II membranes, *Biochemistry 30*, 5379−5387.
18. Baranov, S. V., Tyryshkin, A. M., Katz, D., Dismukes, G. C., Ananyev, G. M., and Klimov, V. V. (2004) Bicabornate is a native cofactor for assembly of the manganese cluster of the photosynthetic water oxidizing complex. Kinetics of reconstitution of O_2 evolution by photoactivation, *Biochemistry 43*, 2070−2079.
19. Miyao, M., and Inoue, Y. (1991) An improved procedure for the photoactivation of photosynthetic oxygen evolution: Effect of artificial electron acceptors on the photoactivation yield of NH_2-OH-treated wheat photosystem II membranes, *Biochim. Biophys. Acta 1056*, 47−56.
20. Liu, B., Shen, P. P., Shi, W., Song, Y. G., Li, W., Nie, Z., and Liu, Y. (2006) Highly efficient photoactivation of Mn-depleted photosystem II by imidazole-liganded manganese complexes, *J. Biol. Inorg. Chem. 11*, 636−632.
21. Han, G., Li, J., Chen, G., Ling, L., Li, S., Khorobrykh, A. A., Zharmukhamedov, S. K., Klimov, V. V., and Kuang, T. (2005) Reconstruction of the water-oxidizing complex in manganese-depleted Photosystem II using synthetic manganese complexes, *J. Photochem. Photobiol., B 81*, 114−120.
22. Bernat, G., Padhye, S., Barta, C., Kovacs, L., and Demeter, S. (2001) Chemical probes for water-oxidation: Synthetic manganese complexes in photoactivation of water splitting complex and as exogenous electron donors to photosystem II, *Z. Naturforsch. C56*, 755−766.
23. Ananyev, G. M., and Dismukes, G. C. (1996) Assembly of the tetra-Mn site of photosynthetic water oxidation by photoactivation: Mn stoichiometry and detection of a new intermediate, *Biochemistry 35*, 4102−4109.
24. Zaltsman, L., Ananyev, G. M., Bruntrager, E., and Dismukes, G. C. (1997) Quantitative kinetic model for photoassembly of the photosynthetic water oxidase from its inorganic constituents: Requirements for manganese and calcium in the kinetically resolved steps, *Biochemistry 36*, 8914−8922.
25. Hwang, H. J., and Burnap, R. L. (2005) Multiflash experiments reveal a new kinetic phase of photosystem II manganese cluster assembly in *Synechocystis* sp. PCC6803 in vivo, *Biochemistry 44*, 9766−9774.
26. Radmer, R., and Cheniae, G. M. (1971) Photoactivation of manganese catalyst of O_2 evolution. 2. Quantum mechanism, *Biochim. Biophys. Acta 253*, 182−186.
27. Pospisil, P., Haumann, M., Dittmer, J., Sole, V. A., and Dau, H. (2003) Stepwise transition of the tetra-manganese complex of photosystem II to a binuclear $Mn_2(\mu\text{-}O)_2$ complex in response to a temperature jump: A time resolved structural investigation employing X-ray absorption spectroscopy, *Biophys. J. 84*, 1370−1386.
28. Barra, M., Haumann, M., and Dau, H. (2005) Specific loss of the extrinsic 18 KDa protein from photosystem II upon heating to 47 °C causes inactivation of oxygen evolution likely due to Ca release from the Mn-complex, *Photosynth. Res. 84*, 231−237.
29. Müller, C., Liebisch, P., Barra, M., Dau, H., and Haumann, M. (2005) The location of calcium in the manganese complex of oxygenic photosynthesis studied by X-ray absorption spectroscopy at the Ca K-edge, *Phys. Scr. T115*, 847−850.
30. Cinco, R. M., McFarlane Holman, K. L., Robblee, J. H., Yano, J., Pizarro, S. A., Bellacchio, E., Sauer, K., and Yachandra, V. K. (2002) Calcium EXAFS establishes the Mn-Ca cluster in the oxygen-evolving complex of photosystem II, *Biochemistry 41*, 12928−12933.
31. Iuzzolino, L., Dittmer, J., Dörner, W., Meyer-Klaucke, W., and Dau, H. (1998) X-ray absorption spectroscopy on layered photosystem II membrane particles suggests manganese-centered oxidation of the oxygen-evolving complex for the S_0-S_1, S_1-S_2, and S_2-S_3 transitions of the water oxidation cycle, *Biochemistry 37*, 17112−17119.
32. Schiller, H., and Dau, H. (2000) Preparation protocols for high-activity photosystem II membrane particles of green algae and higher plants, pH dependence of oxygen evolution and comparison of the S_2-state multiline signal by X-band EPR spectroscopy, *J. Photochem. Photobiol., B 55*, 138−144.
33. Ono, T. A., and Mino, H. (1999) Unique binding site for Mn^{2+} ion responsible for reducing an oxidized YZ tyrosine in manganese-depleted photosystem II membranes, *Biochemistry 38*, 8778−8785.
34. Blubaugh, D. J., and Cheniae, G. M. (1990) Kinetics in hydroxylamine-extracted photosystem II membranes: Relevance to photoactivation and sites of electron donation, *Biochemistry 29*, 5109−5118.
35. Müller, C., Dau, H., and Haumann, M. (2004) Chelex-treatment to obtain highly active PSII membrane particles with minimal Ca-content for XAS at the Ca K-edge, in *Photosynthesis: Fundamental Aspects and Global Perspectives* (Van Est, A., and Bruce, D., Eds.) pp 257−259, International Society of Photosynthesis Research.
36. Ikeuchi, M., and Inoue, Y. (1988) A new 4.8 kDa polypeptide intrinsic to the PSII reaction center, as revealed by modified SDS-PAGE with improved resolution of low-molecular-weight proteins, *Plant Cell Physiol. 29*, 1233−1239.
37. Kashino, Y., Koike, H., and Satoh, K. (2001) An improved sodium dodecyl sulfate polyacrylamide gel electrophoresis system for the analysis of membrane protein complexes, *Electrophoresis 22*, 1004−1007.
38. Laemmli, U. K. (1970) Cleavage of structural proteins during the assembly of the head of bacteriophage T4, *Nature 227*, 680−685.
39. Lowry, O. H., Rosenbrough, A. L., Farr, A. L., and Randall, R. J. (1951) Protein measurement with folin phenol reagent, *J. Biol. Chem. 193*, 265−275.

40. Grabolle, M., and Dau, H. (2005) Energetics of primary and secondary electron transfer in photosystem II membrane particles of spinach revisited on basis of recombination-fluorescence measurements, *Biochim. Biophys. Acta 1708*, 209−218.
41. Clausen, J., Junge, W., Dau, H., and Haumann, M. (2005) Intermediates in photosynthetic water oxidation at high O_2-backpressure detected by chlorophyll delayed fluorescence, *Biochemistry 44*, 12775−12779.
42. Dau, H., Liebisch, P., and Haumann, M. (2004) The structure of the manganese complex of photosystem II in its dark-stable S_1-state-EXAFS results in relation to recent crystallographic data, *Phys. Chem. Chem. Phys. 6*, 4781−4792.
43. Dau, H., Liebisch, P., and Haumann, M. (2003) X-ray absorption spectroscopy to analyze nuclear geometry and electronic structure of biological metal centers: Potential and questions examined with special focus on the tetranuclear manganese complex of oxygenic photosynthesis, *Anal. Bioanal. Chem. 376*, 562−583.
44. Ono, T. A., and Inoue, Y. (1984) Ca^{2+}-dependent restoration of O_2-evolving activity in $CaCl_2$-washed PS II particles depleted of 33, 24 and 16 kDa proteins, *FEBS Lett. 168*, 282−286.
45. Tamura, N., and Cheniae, G. M. (1987) Photoactivation of the water oxidizing complex in Photosystem II membranes depleted of Mn, *Biochim. Biophys. Acta 890*, 179−194.
46. Miller, A. F., and Brudvig, G. W. (1990) Electron-transfer events leading to reconstitution of oxygen-evolution activity in manganese-depleted photosystem II membranes, *Biochemistry 29*, 1385−1392.
47. Ahlbrink, R., Haumann, M., Cherepanov, D., Bögershausen, O., Mulkidjanian, A., and Junge, W. (1998) Function of tyrosine-Z in water oxidation by photosystem II: Electrostatical promotor instead of hydrogen abstractor, *Biochemistry 37*, 1131−1142.
48. Haumann, M., Müller, C., Liebisch, P., Barra, M., Grabolle, M., and Dau, H. (2005) Photosynthetic O_2 formation tracked by time-resolved X-ray experiments, *Science 310*, 1019−1021.
49. Sauer, K., and Yachandra, V. K. (2004) The water-oxidation complex in photosynthesis, *Biochim. Biophys. Acta 1655*, 140−148.
50. Haumann, M., Müller, C., Liebisch, P., Iuzzolino, L., Dittmer, J., Grabolle, M., Neisius, T., Meyer-Klaucke, W., and Dau, H. (2005) Structural and oxidation state changes of the photosystem II manganese complex in four transitions of the water oxidation cycle ($S_0 \rightarrow S_1$, $S_1 \rightarrow S_2$, $S_2 \rightarrow S_3$, $S_{3,4} \rightarrow S_0$) characterized by X-ray absorption spectroscopy at 20 K as well as at room temperature, *Biochemistry 44*, 894−1908.
51. George, G. N., Prince, R. C., and Cramer, S. P. (1989) The manganese site of the photosynthetic water-splitting enzyme, *Science 243*, 789−791.
52. Kirby, J. A., Robertson, A. S., Smith, J. P., Thompson, A. C., Cooper, S. R., and Klein, M. P. (1981) State of manganese in the photosynthetic apparatus. 1. Extended X-ray absorption fine structure studies on chloroplasts and di-μ-oxo-bridged dimanganese model compounds, *J. Am. Chem. Soc. 103*, 5529−5537.
53. Dau, H., Iuzzolino, L., and Dittmer, J. (2001) The tetra-manganese complex of photosystem II during its redox cycle-X-ray absorption results and mechanistic implications, *Biochim. Biophys. Acta 1503*, 24−39.
54. Yano, J., Kern, J., Irrgang, K. D., Latimer, M. J., Bergmann, U., Glatzel, P., Pushkar, Y., Biesiadka, J., Loll, B., Sauer, K., Messinger, J., Zouni, A., and Yachandra, V. K. (2005) X-ray damage to the Mn_4Ca complex in single crystals of photosystem II: A case study for metalloprotein crystallography, *Proc. Natl. Acad. Sci. U.S.A. 102*, 12047−12052.
55. Grabolle, M., Haumann, M., Liebisch, P., Müller, C., and Dau, H. (2006) Rapid loss of structural motifs in the manganese complex of oxygenic photosynthesis by X-ray irradiation at 10−300 K, *J. Biol. Chem. 281*, 4580−4588.
56. Dau, H., and Haumann, M. (2005) Considerations on the mechanism of photosynthetic water oxidation: Dual role of oxo-bridges between Mn ions in (i) redox-potential maintenance and (ii) proton abstraction from substrate water, *Photosynth. Res. 84*, 325−331.
57. Magnuson, A., Liebisch, P., Högblom, J., Anderlund, M., Lomoth, R., Meyer-Klaucke, W., Haumann, M., and Dau, H. (2006) Bridging-type changes facilitate successive oxidation steps at about 1 V in two binuclear manganese complexes: Implications for photosynthetic water oxidation, *J. Inorg. Biochem. 100*, 1234−1243.
58. Meinke, C., Solé, V. A., Pospisil, P., and Dau, H. (2000) Does the structure of the water-oxidizing photosystem II-manganese complex at room temperature differ from its low-temperature? A comparative X-ray absorption study, *Biochemistry 39*, 7033−7040.
59. Zabinsky, S. I., Rehr, J. J., Aukudinov, A., Albers, R. C., and Eller, M. J. (1995) Multiple-scattering calculations of X-ray-absorption spectra, *Phys. Rev. B 52*, 2995−3009.
60. Lomoth, R., Magnuson, A., Sjodin, M., Styring, S., and Hammarstrom, L. (2006) Mimicking the electron donor side of Photosystem II in artificial photosynthesis, *Photosynth. Res. 87*, 25−40.
61. Kuntzleman, T., and Yocum, C. F. (2005) Reduction-induced inhibition and Mn(II) release from the photosystem II oxygen-evolving complex by hydroquinone or NH_2OH are consistent with a Mn(III)/Mn(III)/Mn(IV)/Mn(IV) oxidation state for the dark-adapted enzyme, *Biochemistry 44*, 2129−2149.
62. Seidler, A. (1996) The extrinsic polypeptides of Photosystem II, *Biochim. Biophys. Acta 1277*, 35−60.
63. Freeman, J., Hendry, G., and Wydrzynski, T. (2004) Extraction of the functional manganese and calcium from photosystem II, *Methods Mol. Biol. 274*, 205−215.

BI061842Z